

Compound structure analysis of a new chaotic system

Liu Wenbo¹ Chen Guanrong²

¹ College of Automation Engineering, Nanjing University of Aeronautics and Astronautics, Nanjing 210016, China

² Department of Electronic Engineering, City University of Hong Kong, Hong Kong, China

Abstract: This paper analyzes the compound attractor structure of a new three-dimensional autonomous chaotic system. First, it is found that there exist five equilibria in the chaotic system, and the stabilities of these equilibria are discussed under a constant scalar control input parameter m . Secondly, the trajectories of the attractors on a y - z plane are examined, the reasons why these trajectories can exist or disappear are also described. Finally, the forming procedure of the different scrolls chaotic attractor is explored by computer simulations when the parameter m is varied. It is shown that the new chaotic attractor has a compound structure, it can evolve to other three-dimensional autonomous chaotic systems. The results of theoretical analysis and simulation are helpful for better understanding of other similar chaotic systems.

Key words: three-dimensional autonomous system; chaos; equilibrium; attractor; characteristic equation; compound structure

A new chaotic attractor of a simple three-dimensional continuous-time autonomous system was reported by Liu and Chen^[1]. This new system, albeit structurally simple, has many fairly complex dynamic characteristics, including various periodic orbits (limit cycles), two separate but arbitrarily closely located two-scroll chaotic attractors, and double two-scroll chaotic attractors.

In this paper, we address the question of how these observed phenomena emerge in the new chaotic system, which is useful for understanding and analyzing the new system as well as for designing its electronic circuits. To reveal the essence of the observed emerging phenomena, a tunable scalar control parameter is added to the system, thereby recovering the compound structure and forming procedure of the new chaotic attractor.

The three-dimensional continuous-time autonomous system is described by^[1]

$$\begin{cases} \dot{x} = x - yz \\ \dot{y} = -by + xz \\ \dot{z} = -cz + xy \end{cases} \quad (1)$$

and the “controlled system” with a tunable parameter m is

$$\begin{cases} \dot{x} = x - yz + m \\ \dot{y} = -by + xz \\ \dot{z} = -cz + xy \end{cases} \quad (2)$$

In both systems (1) and (2), parameters b and c satisfy $b > c > 0$ and $b + c > 1$ ^[2].

1 Equilibria: Existence and Stability

The equilibria of system (2) can be easily found,

by solving the three equations $\dot{x} = \dot{y} = \dot{z} = 0$, namely,

$$\begin{cases} x - yz + m = 0 \\ -by + xz = 0 \\ -cz + xy = 0 \end{cases}$$

There are five equilibria for different parameters m .

First, for any value of m , the following equilibrium exists:

$$E_1 = (-m, 0, 0) \quad (3)$$

Secondly, for $0 > m > -\sqrt{bc}$, there are two equilibria:

$$E_{2+} = (x_{2+}, y_{2+}, z_{2+}) = \left(\sqrt{bc}, \sqrt{c + m\sqrt{\frac{c}{b}}}, \sqrt{b + m\sqrt{\frac{b}{c}}} \right) \quad (4)$$

$$E_{2-} = (x_{2-}, y_{2-}, z_{2-}) = \left(\sqrt{bc}, -\sqrt{c + m\sqrt{\frac{c}{b}}}, -\sqrt{b + m\sqrt{\frac{b}{c}}} \right) \quad (5)$$

Finally, for $0 < m < \sqrt{bc}$, the following two equilibria also exist:

$$E_{3+} = (x_{3+}, y_{3+}, z_{3+}) = \left(-\sqrt{bc}, \sqrt{c - m\sqrt{\frac{c}{b}}}, -\sqrt{b - m\sqrt{\frac{b}{c}}} \right) \quad (6)$$

$$E_{3-} = (x_{3-}, y_{3-}, z_{3-}) = \left(-\sqrt{bc}, -\sqrt{c - m\sqrt{\frac{c}{b}}}, \sqrt{b - m\sqrt{\frac{b}{c}}} \right) \quad (7)$$

Equilibria E_{2+} and E_{2-} , and E_{3+} and E_{3-} are symmetric with respect to the x -axis, respectively.

The stabilities of these equilibria are discussed. Linearizing system (2) about its equilibrium E_1 yields the following characteristic equation:

$$f(\lambda) = \lambda^3 + (b + c - 1)\lambda^2 + (bc - c - b - m^2)\lambda - bc + m^2 \quad (8)$$

Denote $A = b + c - 1$, $B = bc - c - b - m^2$, $C = -bc + m^2$ and rewrite (8) as

$$f(\lambda) = \lambda^3 + A\lambda^2 + B\lambda + C = 0 \tag{9}$$

Then, according to the Routh-Hurwitz stability conditions, the real parts of the roots λ are negative if and only if $A > 0$, $B > 0$, $C > 0$ and $AB - C > 0$. So for (8) to be stable, parameter m needs to satisfy the following condition:

$$m^2 < bc - c - b, m^2 > bc \tag{10}$$

Because $b > 0$, $c > 0$, $bc - c - b < bc$, no real value of m can satisfy condition (10), which means that the equilibrium E_1 is always unstable for any value of m .

Similarly, in the case of $m > -\sqrt{bc}$, linearizing system (2) about its other equilibria, E_{2+} and E_{2-} , one obtains the following characteristic equation:

$$f(\lambda) = \lambda^3 + (b + c - 1)\lambda^2 + \left(m\sqrt{\frac{b}{c}} + m\sqrt{\frac{c}{b}} \right)\lambda + 4bc + 4m\sqrt{bc} \tag{11}$$

To satisfy the Routh-Hurwitz conditions for stability, it is required that

$$\left. \begin{aligned} m > 0 \\ (b + c - 1)m\left(\sqrt{\frac{b}{c}} + \sqrt{\frac{c}{b}}\right) - 4bc - 4m\sqrt{bc} > 0 \end{aligned} \right\} \tag{12}$$

This is satisfied only if

$$\left. \begin{aligned} (b - c)^2 > b + c \\ m > \frac{4b^2c^2}{(b - c)^2 - (b + c)} \end{aligned} \right\} \tag{13}$$

and in this case, the equilibria E_{2+} and E_{2-} are stable; otherwise, these two equilibria are unstable.

Similarly, linearizing system (2) about the other equilibria, E_{3+} and E_{3-} , in the case of $m < \sqrt{bc}$, yields the following characteristic equation:

$$f(\lambda) = \lambda^3 + (b + c - 1)\lambda^2 - \left(m\sqrt{\frac{b}{c}} + m\sqrt{\frac{c}{b}} \right)\lambda + 4bc - 4m\sqrt{bc} \tag{14}$$

and, as analyzed above, these two equilibria are stable only when

$$\left. \begin{aligned} (b - c)^2 > b + c \\ m < \frac{-4b^2c^2}{(b - c)^2 - (b + c)} \end{aligned} \right\} \tag{15}$$

otherwise, they are unstable.

2 Trajectory Analysis: on the y - z Plane

Consider the second and the third equations of system (2):

$$\begin{cases} \dot{y} = -by + xz \\ \dot{z} = -cz + xy \end{cases} \tag{16}$$

where $b > c > 0$, and y, z are state variables while x is considered as a known function of the time variable t .

In particular, when x is a constant, independent of y, z and t , system (16) can be regarded as a two-dimensional linear system with constant coefficients^[3]. When $x(t)$ goes through the intervals $(-\infty, -\sqrt{bc}]$, $[-\sqrt{bc}, \sqrt{bc}]$ and $[\sqrt{bc}, +\infty)$, system (16) will have different dynamical behaviors, leading to very complex dynamics.

The trajectories of system (16) on the y - z plane are now examined in detail. First, examine the two lines passing through the origin corresponding to the transformed axes which the trajectories are tangent to. These lines have the form $z = ky$. To determine the values of k , one may use the first equation to divide the second equation in system (16) and then obtain^[4]:

$$\frac{dz}{dy} = \frac{dz/dt}{dy/dt} = \frac{-cz + xy}{-by + xz} \tag{17}$$

Substituting $z = ky$, we obtain

$$k = \frac{-cky + xy}{-by + xky} = \frac{-ck + x}{-b + kx}$$

Solving for k yields

$$k = \frac{(b - c) \pm \sqrt{(b - c)^2 + 4x^2}}{2x} \tag{18}$$

If let

$$\mu = \frac{b - c}{2x} \tag{19}$$

then Eq.(18) can be rewritten as

$$k = \mu \pm \sqrt{1 + \mu^2} \tag{20}$$

If $x \in (0, +\infty)$, let $k_1 = \mu + \sqrt{1 + \mu^2}$, $k_2 = \mu - \sqrt{1 + \mu^2}$, then $\mu \in (0, +\infty)$, and hence $k_1 \in (1, +\infty)$, $k_2 \in (-1, 0)$. It is now clear that the two transformed axes are $z = k_1y$ and $z = k_2y$, as shown by the two real lines in Fig.1. Similarly, if $x \in (-\infty, 0)$, let $k'_1 = \mu + \sqrt{1 + \mu^2}$, $k'_2 = \mu - \sqrt{1 + \mu^2}$, then $\mu \in (-\infty, 0)$, and $k'_1 \in (0, 1)$, $k'_2 \in (-\infty, -1)$. Hence, the two transformed axes are $z = k'_1y$ and $z = k'_2y$, as shown by the two dashed lines in Fig.1.

Because $b > c > 0$ in system (2) or system (16), for any x , it is easy to prove that the system trajectories on the y - z plane will be confined within

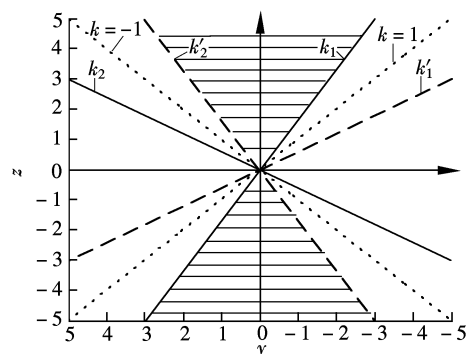


Fig.1 Trajectories domains of system (2) on the y - z plane

the domain of $|z(t)| > |y(t)|$ [5].

Hence, by combining the above conditions, one can see that the trajectories of system (16) on the y - z plane will be confined within the shadowy domain shown in Fig.1, regardless of the variable x , and the two borderlines are given by $z = k_{1e}y$ and $z = k'_{2e}y$.

On the other hand, for any equilibrium of system (2), the slopes of these two lines on the y - z plane, which pass through the origin and equilibria, are independent of m :

$$k_{1e} = \frac{z_{2+}}{y_{2+}} = \frac{z_{2-}}{y_{2-}} = \frac{\sqrt{b+m}\sqrt{b/c}}{\sqrt{c+m}\sqrt{c/b}} = \sqrt{\frac{b}{c}} > 1$$

$$k_{2e} = \frac{z_{3+}}{y_{3+}} = \frac{z_{3-}}{y_{3-}} = -\frac{\sqrt{b-m}\sqrt{b/c}}{\sqrt{c-m}\sqrt{c/b}} = -\sqrt{\frac{b}{c}} < -1$$

From the above, one can see that if any chaotic attractor exists, then on the y - z plane the equilibrium must be inside the shadowy area in Fig.1 [5]. Next, the existence of equilibria as attractors are discussed when the parameter m is varied.

For system (2), let $k_{1\min} = \mu_{\min} + \sqrt{1 + u_{\min}^2}$, $k'_{2\max} = \mu_{\max} - \sqrt{1 + u_{\max}^2}$, where $\mu_{\min} = (\sqrt{b} + \sqrt{c})/x_{\max} > 0$, when $x > 0$; $\mu_{\max} = (\sqrt{b} + \sqrt{c})/x_{\min} < 0$, when $x < 0$. Because system (2) is symmetric to the x -axis, but it is not symmetric to the y -axis or z -axis, one can see that $|x_{\min}| \neq x_{\max}$ in the case of $m \neq 0$, but $|x_{\min}| < x_{\max}$ when $m > 0$ and $|x_{\min}| > x_{\max}$ when $m < 0$.

For equilibria E_{2+} , E_{2-} and E_{3+} , E_{3-} , on the y - z plane, they are located on the lines $z = k_{1e}y$ and $z = k_{2e}y$, respectively. If they exist as attractors, they must satisfy the following necessary conditions:

$$\frac{z_{2+}}{y_{2+}} = \frac{z_{2-}}{y_{2-}} = k_{1e} = \sqrt{\frac{b}{c}} > k_{1\min} \quad \text{when } m \geq -\sqrt{bc}$$

$$\frac{z_{3+}}{y_{3+}} = \frac{z_{3-}}{y_{3-}} = k_{2e} = -\frac{b}{c} > k'_{2\max} \quad \text{when } m < \sqrt{bc}$$

When $m > 0$, with the increase of m , both x_{\max} and x_{\min} will increase, but both $k_{1\min}$ and $k'_{2\max}$ become smaller where $k_{1\min}$ will be close to 1 and $k'_{2\max}$ will be far away from -1 . The upper-shadowy section in Fig.1 will circumsolve to the right and the down-shadowy section, to the left.

Hence, at $m = 0$, if two attractors around the equilibria E_{2+} and E_{2-} exist, respectively, then they will still remain to exist for all $\sqrt{bc} > m > 0$. But for the other two equilibria E_{3+} and E_{3-} , the situation is different: the part of the trajectories around the two equilibria, respectively, will not satisfy condition $|z(t)| > |k'_{2\max}y(t)|$. In this case, with the increase of m , the trajectories around the two equilibria

respectively will become less dense and the attractors also become smaller in size (see Fig.3(a)). Finally, all the trajectories disappear, and so do the two attractors (see Fig.4(a)).

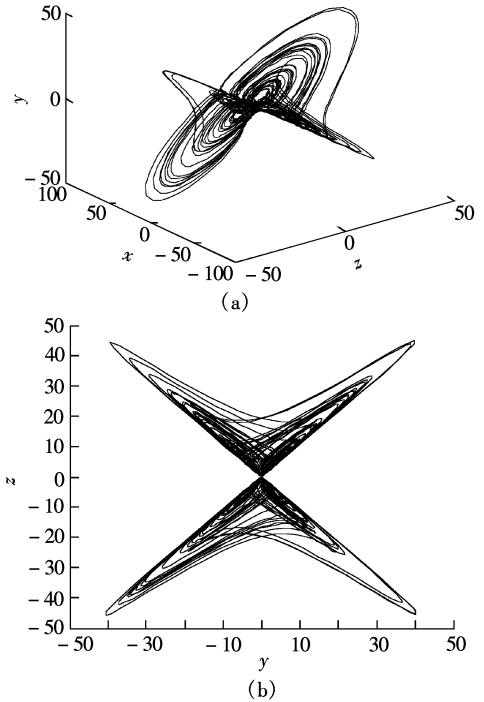


Fig.2 Chaotic attractor with $m = 0$. (a) Three-dimensional view; (b) Projection on the y - z plane

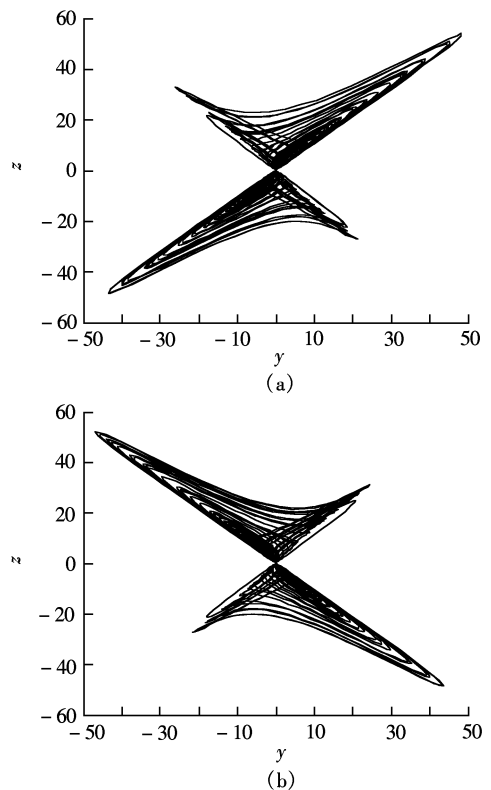


Fig.3 Chaotic attractor with $m = \pm 6.9$. (a) Projection on the y - z plane with $m = 6.9$; (b) Projection on the y - z plane with $m = -6.9$

Similarly, in the domain of $0 > m > -\sqrt{bc}$, with the decrease of m , the two attractors around the two equilibria E_{2+} and E_{2-} , respectively, will eventually disappear (see Fig.3(b) and Fig.4(b)).

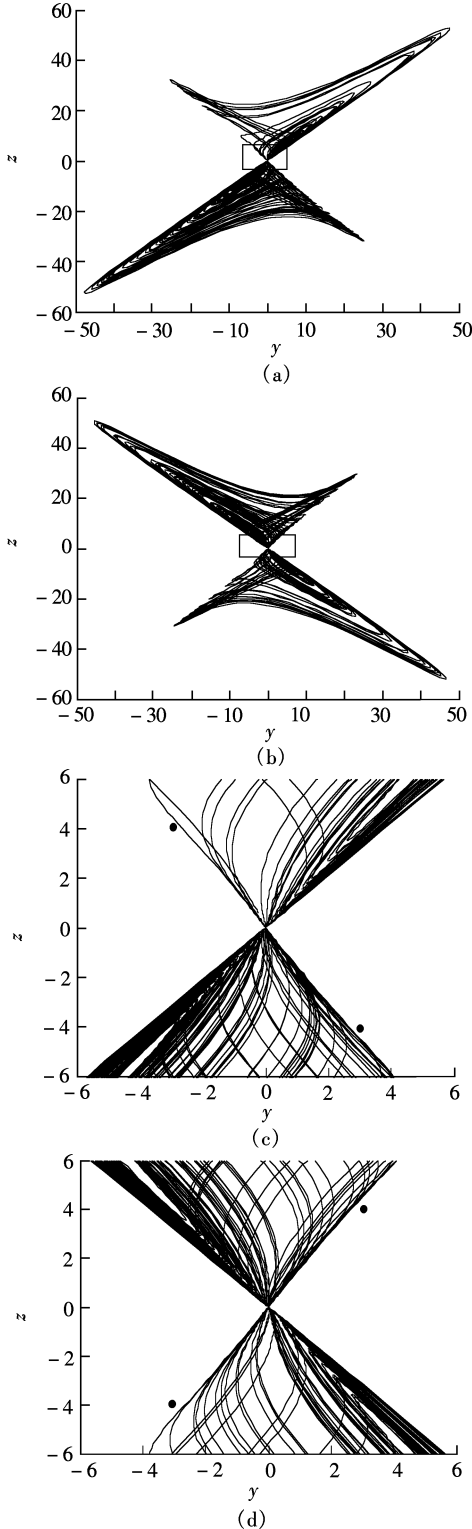


Fig.4 Chaotic attractor with $m = \pm 7.5$. (a) Projection on the y - z plane with $m = 7.5$; (b) Projection on the y - z plane with $m = -7.5$; (c) Zoom figure of Fig.4 (a); (d) Zoom figure of Fig.4 (b)

3 Forming Procedure of the New Attractor and Its Compound Structure

Return to system (2). Now, let parameters $b = 16$, $c = 9$ in the system to show the forming procedure of the new attractor and to reveal its compound structure through numerical simulations. The system now becomes

$$\begin{cases} \dot{x} = x - yz + m \\ \dot{y} = -16y + xz \\ \dot{z} = -9z + xy \end{cases} \quad (21)$$

From the above analysis, it is known that the five equilibria of system (21) are

$$E_1 = (-m, 0, 0)$$

When $0 > m > -12$,

$$E_{2+} = \left(12, \sqrt{9 + \frac{3}{4}m}, \sqrt{16 + \frac{4}{3}m} \right)$$

$$E_{2-} = \left(12, -\sqrt{9 + \frac{3}{4}m}, -\sqrt{16 + \frac{4}{3}m} \right)$$

When $0 < m < 12$,

$$E_{3+} = \left(-12, \sqrt{9 - \frac{3}{4}m}, -\sqrt{16 - \frac{4}{3}m} \right)$$

$$E_{3-} = \left(-12, -\sqrt{9 - \frac{3}{4}m}, \sqrt{16 - \frac{4}{3}m} \right)$$

And

$$\frac{z_{2+}}{y_{2+}} = \frac{z_{2-}}{y_{2-}} = k_{1e} = \sqrt{\frac{b}{c}} = \frac{4}{3}$$

$$\frac{z_{3+}}{y_{3+}} = \frac{z_{3-}}{y_{3-}} = k_{2e} = -\sqrt{\frac{b}{c}} = -\frac{4}{3}$$

When $m = 0$, the phase portraits of system (21) are shown in Fig.2. When $m = 6.9$ and $m = -6.9$, the phase portraits of system (21) are shown in Fig.3. In Figs.3 (a) and (b), one can see that the trajectories around the equilibria E_{3+} , E_{3-} and E_{2+} , E_{2-} , respectively, become less dense, and if one continues to increase the absolute value of m , then the system trajectories around these equilibria will disappear as shown in Fig.4. Figs.4 (c) and (d) are the zoom figures near the origin in Figs.4 (a) and (b), respectively, where the dots are the equilibria. When one continues to increase the absolute value of m , system trajectories on the y - z plane will move to the origin $(0, 0)$, and thus cannot travel to the hyper-plane of $z = 0$ even under small perturbation^[5]. So, one of the attractors shown in Fig.4 will disappear, and there will remain only one attractor (either upper-attractor or down-attractor according to the initial value) on the phase space, which also shows some periodic orbits when parameter $|m|$ is very large, as shown in Fig.5.

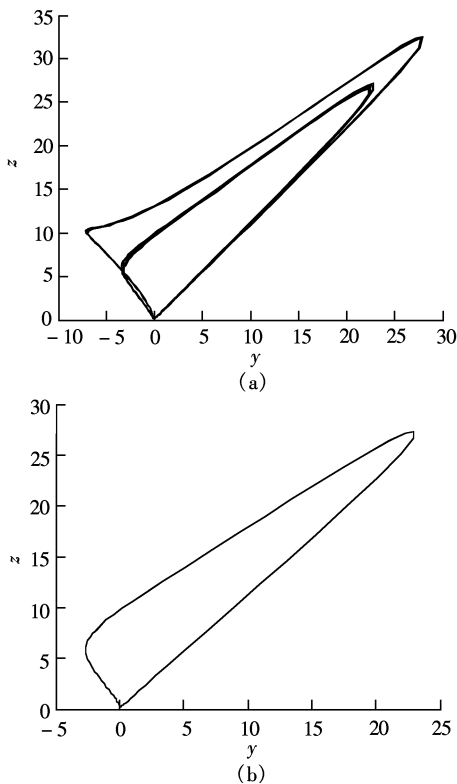


Fig.5 Periodic orbits. (a) $m = 14$; (b) $m = 30$

4 Conclusion

This paper studies the dynamic properties and the forming procedure of the new chaotic attractor. It is shown that the new chaotic attractor has a compound structure, which is similar to the Lorenz, Lorenz-like, and Chen's attractors^[6-9]. By tuning a scalar parameter as a control input, one can obtain one-scroll, two-scroll and double two-scroll chaotic attractors as well as limit cycles in the system. Naturally, there are still some interesting issues about

such compound structures of attractors, which deserve further investigation in the future for deeper understand of various chaotic systems.

References

- [1] Liu W B, Chen G. A new chaotic system and its generation [J]. *International Journal of Bifurcation and Chaos*, **2003**, *13*(1): 261 - 267.
- [2] Liu W B, Chen G. Dynamical analysis of a 4-scroll chaotic attractor [J]. *International Journal of Bifurcation and Chaos*, **2004**, *14*(3): 971 - 998.
- [3] Lü J, Chen G. Dynamical analysis of a new chaotic attractor [J]. *International Journal of Bifurcation and Chaos*, **2002**, *12*(5): 1001 - 1015.
- [4] Nagle R K, Saff E B. *Fundamentals of differential equations and boundary value problems* [M]. New York: Addison Wesley, 1994.
- [5] Liu W B, Chen G. Can a three-dimensional smooth autonomous quadratic chaotic system generate a single four-scroll attractor? [J]. *International Journal of Bifurcation and Chaos*, **2004**, *14*(4): 1395 - 1403.
- [6] Lü J, Chen G, Zhang S. The compound structure of a new chaotic attractor [J]. *Chaos Solitons and Fractals*, **2002**, *14*(5): 669 - 672.
- [7] Lü J, Zhou T, Chen G, et al. The compound structure of Chen's attractor [J]. *International Journal of Bifurcation and Chaos*, **2002**, *12*(4): 855 - 858.
- [8] Elwakil A, Kennedy M P. Construction of classes of circuit-independent chaotic oscillators using passive-only nonlinear devices [J]. *IEEE Trans Circuits Syst — I*, **2001**, *48*(3): 289 - 307.
- [9] Ozoguz S, Elwakil A, Kennedy M P. Experimental verification of the butterfly attractor in a modified Lorenz system [J]. *IEEE Trans Circuits Syst — I*, **2002**, *49*(4): 527 - 530.

一种新的混沌系统的复合结构分析

刘文波

陈关荣

(南京航空航天大学自动化学院, 南京 210016) (香港城市大学电子工程系, 中国香港)

摘要: 分析了一种新的三维自治混沌系统吸引子的复合结构. 首先证明了该混沌系统存在 5 个平衡点, 讨论了系统的控制参数大小同平衡点稳定性之间的关系. 其次, 对吸引子在 $y-z$ 平面的运动轨迹作了理论分析, 描述了吸引子存在及消失的原因. 最后, 通过对该混沌系统运动轨迹在不同控制参数作用下的计算机仿真, 揭示了涡卷数不同的混沌吸引子形成的过程. 表明该混沌系统具有复合结构, 能够演化成其他的三维自治混沌系统. 理论分析及仿真结果对分析其他具有相似结构的混沌系统具有重要的参考价值.

关键词: 三维自治系统; 混沌; 平衡点; 吸引子; 特征方程; 复合结构

中图分类号: O415.5